Doping effects of Sb and Pb in epitaxial topological insulator Bi_2Se_3 thin films: An *in situ* angle-resolved photoemission spectroscopy study

Yi Zhang,[1] Cui-Zu Chang,[1,2] Ke He,[1,a)] Li-Li Wang,[1] Xi Chen,[2] Jin-Feng Jia,[2] Xu-Cun Ma,[1,b)] and Qi-Kun Xue[1,2]
[1]*Institute of Physics, Chinese Academy of Sciences, Beijing 100190, People's Republic of China*
[2]*Department of Physics, Tsinghua University, Beijing 100084, People's Republic of China*

(Received 17 August 2010; accepted 21 October 2010; published online 11 November 2010)

Bi_2Se_3 is a typical three-dimensional topological insulator but always exhibits metallic behavior due to heavy n-type doping. With *in situ* angle-resolved photoemission spectroscopy, we have systematically studied the doping effects of Sb and Pb on the electronic structure of Bi_2Se_3 films prepared by molecular beam epitaxy. The surface chemical potential of Bi_2Se_3 can be tuned by 110 and 145 meV by doping Sb and Pb atoms, respectively. By codoping Pb and Sb, the Fermi level can be shifted from above to below the Dirac point. The underlying mechanism in different doping effects of Sb and Pb is discussed. © *2010 American Institute of Physics*. [doi:10.1063/1.3516160]

Topological insulators (TIs)[1–10] are insulating in bulk but host metallic surface/edge states, which are protected by the topological characters of the bulk bands. This class of materials has recently attracted great attention due to their exotic physical properties and potential applications in spintronics and topological quantum computation. Bi_2Se_3 is one of the most studied three-dimensional TIs for its relatively large gap and simple nontrivial surface band structure.[11–13] Tuning the chemical potential, especially that near surface region, is of crucial importance to the investigations and applications of TIs since most of the predicted exotic properties of TIs come from the Dirac-type surface states and strongly depend on the relative position between Fermi level and Dirac point.[1,2] Bi_2Se_3 bulk crystals are always heavily n-type doped due to selenium vacancies and other defects.[12,13] Progress has been made in tuning the chemical potential of Bi_2Se_3 bulk crystals by chemical doping[13–15] and field effect.[16–18] In Sb-doped Bi_2Se_3, a carrier density as low as 2.9×10^{-16} cm^{-3} has been reported.[15] In earlier studies, by codoping Sb and Pb, p-type Bi_2Se_3 has been realized.[19]

In this work, by *in situ* angle-resolved photoemission spectroscopy (ARPES), we have systematically investigated the effects of Sb and Pb doping in Bi_2Se_3 films grown by molecular beam epitaxy (MBE) on the chemical potential near surface. This way, we could monitor the band evolution as a function of dopant concentration. It is found that Sb and Pb exhibit different doping behaviors. More importantly, by codoping the two elements, the surface chemical potential of Bi_2Se_3 film can be changed by as much as 255 meV, which shifts the Fermi level below the Dirac point. The results provide useful information on preparing desired materials for transport measurement of topological features and exploring the application of TIs.

The experiments were preformed in an ultrahigh vacuum system ($<1.5\times10^{-10}$ Torr) that consists of an MBE growth chamber, a scanning tunneling microscope (STM) (Omicron) and an ARPES spectrometer (VG-Scienta). The substrate for thin film sample growth is bilayer-graphene-terminated 6H-SiC (0001).[20,21] High purity Bi (99.9999%), Se (99.999%), Sb (99.9999%), and Pb (99.9999%) were used, and they were evaporated from standard Knudsen cells. All the films used in this work have a thickness of 20 quintuple-layers (QLs). The photons used in ARPES measurement are unpolarized He-Iα (21.21 eV) produced by a Gammadata VUV discharging lamp. A Scienta SES-2002 analyzer was used to collect the photoelectrons. All the ARPES data were taken at room-temperature.

$Bi_{2-x-y}Sb_xPb_ySe_3$ films were grown under Se-rich conditions, which can significantly reduce Se vacancies in the films.[21] When the Se source temperature is lower than that of the substrate, the deposition rate is only dependent on the flux of Bi (Sb and Pb), which have a low vapor pressure.[21] Therefore, the concentration of doping can simply be controlled by the flux ratio of Bi, Sb, and Pb, which relates to the source temperature (T) via $J\propto P/\sqrt{T}$,[22] where J is the beam flux and P is the vapor pressure at that source temperature T. J at different evaporation temperatures can be calculated by a calibrated flux J_0 at a certain temperature T_0,

$$J = J_0\frac{P}{P_0}\sqrt{\frac{T_0}{T}}. \quad (1)$$

J_0 was calibrated by STM[23,24] and reflective high-energy electron diffraction (RHEED) oscillation.[24] In the present work, the substrate temperature was kept at 220 °C in $Bi_{2-x-y}Sb_xPb_ySe_3$ growth. The source temperatures of Bi and Se were 520 and 150 °C, respectively, with a Bi/Se flux ratio

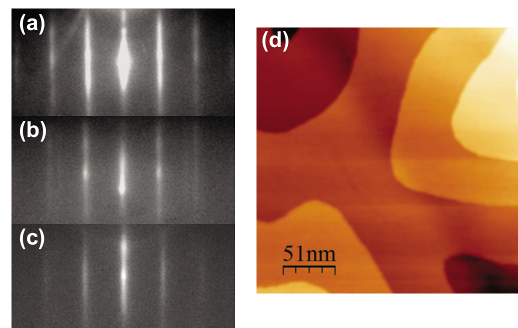

FIG. 1. (Color online) RHEED patterns of (a) 20QL Bi_2Se_3 film, (b) $Bi_{1.7}Sb_{0.3}Se_3$ film, (c) and $Bi_{1.6963}Sb_{0.3}Pb_{0.0037}Se_3$ film grown on bilayer-graphene-terminated 6H-SiC(0001) by MBE. (d) STM image of 20 QL $Bi_{1.5}Sb_{0.5}Se_3$ film with bias of +1.500 V and tunneling current of 0.02 nA.

[a)]Electronic mail: kehe@aphy.iphy.ac.cn.
[b)]Electronic mail: xcma@aphy.iphy.ac.cn

 © 2010 American Institute of Physics

Downloaded 30 Dec 2010 to 166.111.26.101. Redistribution subject to AIP license or copyright; see http://apl.aip.org/about/rights_and_permissions

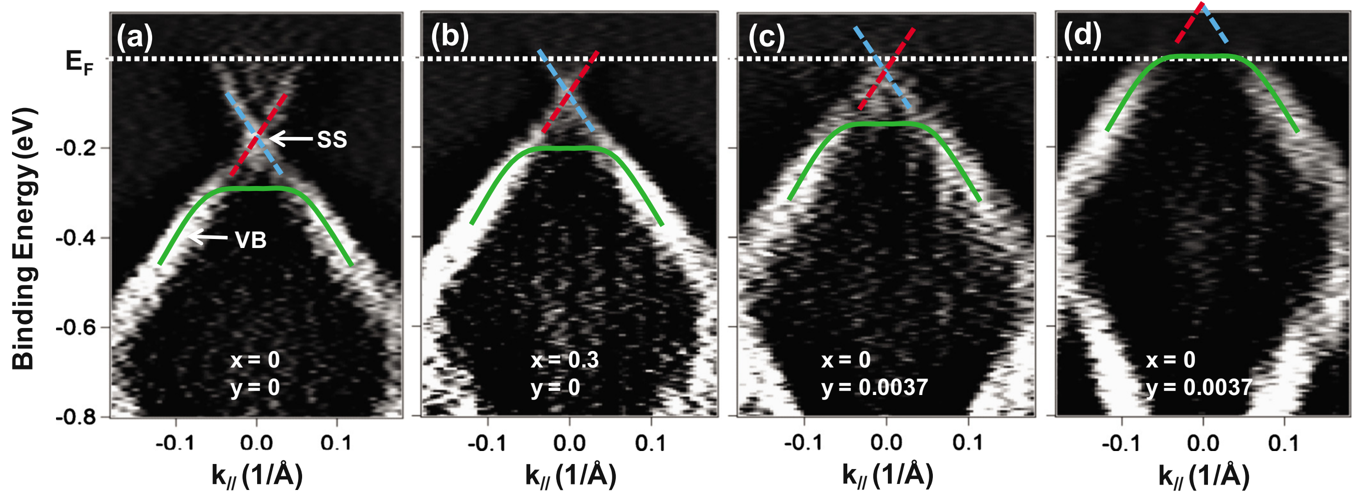

FIG. 2. (Color online) Second-order differential ARPES spectra of 20 QL $Bi_{2-x-y}Sb_xPb_ySe_3$ films along $\bar{\Gamma}-\bar{K}$ direction: (a) bare Bi_2Se_3 film, (b) $Bi_{1.7}Sb_{0.3}Se_3$ film, (c) $Bi_{1.9963}Pb_{0.0037}Se_3$ film, and (d) $Bi_{1.6963}Sb_{0.3}Pb_{0.0037}Se_3$ film. The solid lines indicate the tops of VBs. The dashed lines indicate the Dirac-cone-like SSs. The Fermi level is indicated by the dotted line.

of 1:15 and a growth rate of 0.14 QL/min. The evaporation temperature of Sb from 340 to 380 °C leads to a Sb concentration (x) from 0.18 to 0.75, and the temperature of Pb from 350 to 420 °C leads to a Pb concentration (y) from 1×10^{-4} to 0.15.

Figures 1(a)–1(c) show the RHEED patterns of a bare Bi_2Se_3 film, a Sb-doped Bi_2Se_3 film, and a Bi_2Se_3 film codoped by Sb and Pb, respectively. The Sb and Pb concentrations correspond to the optimized values for chemical doping, as will be addressed below. The sharp 1×1 streaks in all of the patterns demonstrate that the crystallographic structure and quality of the epitaxial Bi_2Se_3 films are little influenced by Sb/Pb doping.[19,25] Figure 1(d) shows a STM image of $Bi_{1.5}Sb_{0.5}Se_3$ films. The uniform and atomic flat terraces indicate that the doped atoms are homogeneously diffused into Bi_2Se_3 matrix instead of segregating into clusters. ARPES band maps (second-order differential spectra are used) of $Bi_{2-x-y}Sb_xPb_ySe_3$ films with different doping levels are shown in Figs. 2(a)–2(d). The bands indicated by dashed red and blue lines correspond to the Dirac-cone-like surface states (SSs), and the features with solid green lines are tops of the valence bands (VBs).[20] The bands exhibit essentially a similar structure and dispersion except that their positions relative to the Fermi level (E_F) are different. In the bare Bi_2Se_3 [Fig. 2(a)], the Dirac point is located at $E_B=-0.170$ eV (E_B is the binding energy), and the film is n-type. By doping Sb [x(Sb)=0.3, y(Pb)=0], both surface and valence bands are shifted toward the Fermi level [see Fig. 2(b)], which suggests that the film is depleted with electrons. The Dirac point is moved to $E_B=-0.06$ eV. Doping Pb atoms can also shift the band. Figure 2(c) shows the spectra of a Pb-doped film (x=0, y=0.0037). The Dirac point is shifted to $E_B=-0.025$ eV. Codoping Sb and Pb atoms in Bi_2Se_3 film [see Fig. 2(d)] makes the Dirac point shifted to above the Fermi level.

The Dirac point positions of $Bi_{2-x-y}Sb_xPb_ySe_3$ films, as a function of Sb/Pb concentration, are shown in Fig. 3. For the samples with Dirac point above the Fermi level, we calculated the position of Dirac point with the top of valence band since the band dispersion does not change with Sb/Pb doping. Figure 3(a) shows the dependence of the Dirac point position on the Sb concentration. We can see that as Sb concentration increases the Dirac point moves toward the Fermi level until x=0.3 where the Dirac point is shifted by about 110 meV from bare Bi_2Se_3. Additional Sb doping makes the

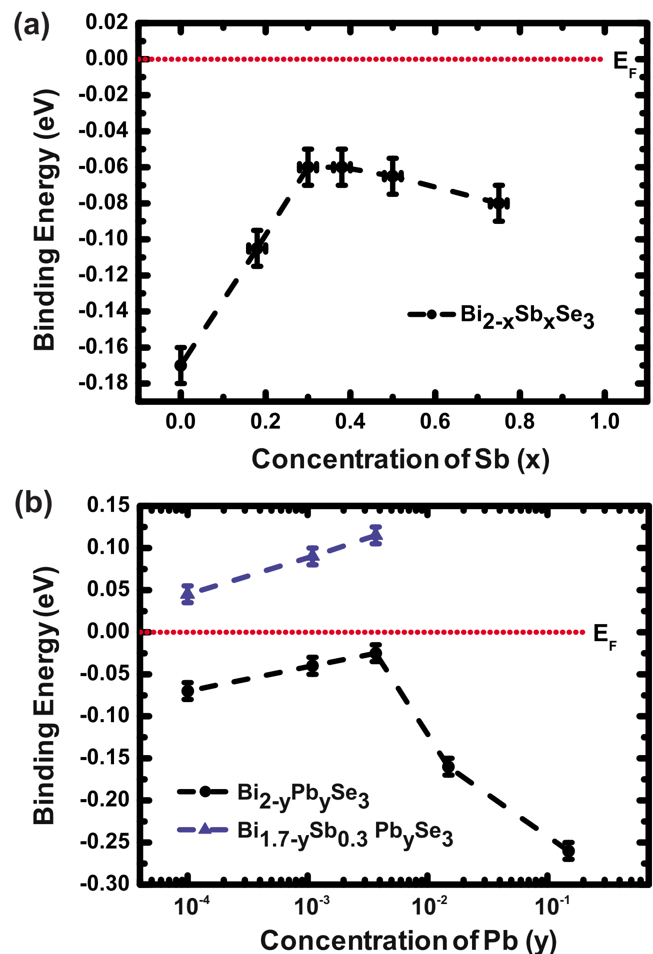

FIG. 3. (Color online) The dependences of the Dirac point positions of (a) 20 QL $Bi_{2-x}Sb_xSe_3$ film, (b) 20 QL $Bi_{2-y}Pb_ySe_3$ film [the data points below E_F in (b)] and 20 QL $Bi_{1.7-y}Sb_{0.3}Pb_ySe_3$ film [the data points above E_F in (b)] on Sb/Pb concentration x/y. The coordinate of Pb concentration y in (b) is logarithmic. The Fermi level is indicated by the dotted lines.

Downloaded 30 Dec 2010 to 166.111.26.101. Redistribution subject to AIP license or copyright; see http://apl.aip.org/about/rights_and_permissions

Dirac point move away from the Fermi level. At the same time the ARPES spectra become blur and completely disappear for x ~ 0.75, suggesting that the crystalline structure is greatly interrupted. In the Pb case [black dots in Fig. 3(b)], at y=0.0037 the Dirac point reaches its maximal value, approximately at 145 meV above that of bare Bi_2Se_3. The blue dots in Fig. 3(b) show the Pb concentration dependence of the Dirac point position of the optimally Sb-doped Bi_2Se_3 films (x=0.3). We can find that the evolution is basically similar to the Pb case except for an additional shift of ~110 meV.

Interestingly, Sb and Pb exhibit different doping behaviors in Bi_2Se_3 films. For Sb, below the optimal concentration (x=0.3), the energy shift is linearly dependent on Sb concentration. However, Pb exhibits a logarithmical behavior [note the logarithmic coordinate used in Fig. 3(b)]. The result suggests that Sb and Pb have different doping mechanisms in Bi_2Se_3.

Lead is divalent[19] in Bi_2Se_3, and thus each Pb atom introduces one hole by substitution for trivalent Bi atom.[19,26] Our ARPES data show that for the undoped Bi_2Se_3 film, the Fermi level basically lies in the energy gap. Similar to a conventional semiconductor, the carrier density (n) and E_F are related by the formula[27]

$$\left(\frac{n}{N_{\text{eff}}^C}\right)e^{E_C/k_BT} = e^{E_F/k_BT}, \tag{2}$$

where E_C is the energy of the conduction band minimum (CBM) and N_{eff}^C is the density of states at CBM. In this case, the Fermi energy is logarithmically dependent on carrier density n, which can account for the observed logarithmical relation between band shift and Pb concentration in Fig. 3(b).

The linear dependence in the case of Sb doping suggests that Sb does not directly contribute carriers in Bi_2Se_3 like Pb. Sb and Bi belong to the same group in the periodic table, and thus in principle, the substitution of Sb for Bi in Bi_2Se_3 will not introduce additional charges. The n-type doping in Bi_2Se_3 is mainly due to Se vacancies,[14,19] which result from Se segregation at the surfaces. So, it is likely that Sb substitution reduces the n-type carriers by suppressing Se vacancies, as proposed in previous studies.[25,28] Sb atoms reduce the unit cell volume when doped in Bi_2Se_3, which might increase the formation energy of Se vacancies (E_v).[18,28] E_v in first approximation is linearly related to the concentration of Sb atoms.[28] The vacancy density n_v is exponentially related with E_v due to Boltzmann distribution. The carrier density n is exponentially dependent on the Fermi energy as shown in Eq. (2) and also on E_v since it is proportional to n_v. So, the linear relation between Sb concentration and energy shift is obtained.

It is worthy to note that since ARPES is surface sensitive and the chemical potential at surface and inside of a film may be different due to band bending, the bulk carrier density of a Sb- and Pb-doped Bi_2Se_3 film cannot be directly obtained from the data shown in Fig. 3. Transport results from previous works as well as from ours have shown that the bulk carriers of Bi_2Se_3 can also be tuned from n- to p-type by codoping of Sb and Pb. We can expect that bulk chemical potential shows similar concentration dependent behavior to that shown in Fig. 3 but with an additional energy shift induced by band bending. Modulation doping of Sb and Pb in different layers of a Bi_2Se_3 film could be used to tune bulk and surface chemical potentials independently.

In conclusion, the doping effects of Sb and Pb atoms on the surface chemical potential of MBE grown Bi_2Se_3 films were systematically studied by ARPES. The optimized concentrations for both dopants were found, and conversion of surface region from n- to p-doped was realized. The quantitative analysis of the relationship between band shift and doping concentration reveals the different mechanisms of Sb and Pb doping.

This work was supported by NSFC (Grant Nos. 10974237 and 10721404) and Ministry of Science and Technology of China (Grant No. 2009CB929400).

[1] X. L. Qi and S. C. Zhang, Phys. Today **63** (1), 33 (2010).
[2] M. Z. Hasan and C. L. Kane, e-print arXiv:1002.3895 (2010).
[3] J. E. Moore, Nature (London) **464**, 194 (2010).
[4] B. A. Bernevig, T. L. Hughes, and S. C. Zhang, Science **314**, 1757 (2006).
[5] L. M. König, S. Wiedmann, C. Brüne, A. Roth, H. Buhmann, L. W. Molenkamp, X. L. Qi, and S. H. Zhang, Science **318**, 766 (2007).
[6] L. Fu, C. L. Kane, and E. J. Mele, Phys. Rev. Lett. **98**, 106803 (2007).
[7] D. Hsieh, D. Qian, L. Wray, Y. Xia, Y. S. Hor, R. J. Cava, and M. Z. Hasan, Nature (London) **452**, 970 (2008).
[8] X. L. Qi, T. L. Hughes, and S. C. Zhang, Phys. Rev. B **78**, 195424 (2008).
[9] D. Hsieh, Y. Xia, L. Wray, D. Qian, A. Pal, J. H. Dil, J. Osterwalder, F. Meier, G. Bihlmayer, C. L. Kane, Y. S. Hor, R. J. Cava, and M. Z. Hasan, Science **323**, 919 (2009).
[10] A. Nishide, A. A. Taskin, Y. Takeichi, T. Okuda, A. Kakizaki, T. Hirahara, K. Nakatsuji, F. Komori, Y. Ando, and I. Matsuda, Phys. Rev. B **81**, 041309 (2010).
[11] H. J. Zhang, C. X. Liu, X. L. Qi, X. Dai, Z. Fang, and S. C. Zhang, Nat. Phys. **5**, 438 (2009).
[12] Y. Xia, D. Qian, D. Hsieh, L. Wray, A. Pal, H. Lin, A. Bansil, D. Grauer, Y. S. Hor, R. J. Cava, and M. Z. Hasan, Nat. Phys. **5**, 398 (2009).
[13] D. Hsieh, Y. Xia, D. Qian, L. Wray, J. H. Dil, F. Meier, J. Osterwalder, L. Patthey, J. G. Checkelsky, N. P. Ong, A. V. Fedorov, H. Lin, A. Bansil, D. Grauer, Y. S. Hor, R. J. Cava, and M. Z. Hasan, Nature (London) **460**, 1101 (2009).
[14] Y. S. Hor, A. Richardella, P. Roushan, Y. Xia, J. G. Chekelsky, A. Yazdani, M. Z. Hasan, N. P. Ong, and R. J. Cava, Phys. Rev. B **79**, 195208 (2009).
[15] J. G. Analytis, R. D. McDonald, S. C. Riggs, J.-H. Chu, G. S. Boebinger, and I. R. Fisher, e-print arXiv:1003.1713 (2010).
[16] J. Chen, H. J. Qin, F. Yang, J. Liu, T. Guan, F. M. Qu, G. H. Zhang, J. R. Shi, X. C. Xie, C. L. Yang, K. H. Wu, Y. Q. Li, and L. Lu, Phys. Rev. Lett. **105**, 176602 (2010).
[17] J. G. Checkelsky, Y. S. Hor, R. J. Cava, and N. P. Ong, e-print arXiv:1003.3883 (2010).
[18] D. S. Kong, W. H. Dang, J. J. Cha, H. Li, S. Meister, H. L. Peng, Z. F. Liu, and Y. Cui, Nano Lett. **10**, 2245 (2010).
[19] J. Kašparová, Č. Drašar, and A. Krejčová, J. Appl. Phys. **97**, 103720 (2005).
[20] Y. Zhang, K. He, C. Z. Chang, C. L. Song, L. L. Wang, X. Chen, and J. J. Jia, Z. Fang, X. Dai, W. Y. Shan, S. Q. Shen, Q. Niu, X. L. Qi, S. C. Zhang, X. C. Ma, and Q. K. Xue, Nat. Phys. **6**, 584 (2010).
[21] C. L. Song, Y. L. Wang, Y. P. Jiang, Y. Zhang, C. Z. Chang, L. L. Wang, K. He, X. Chen, J. F. Jia, Y. Y. Wang, Z. Fang, X. Dai, X. C. Xie, X. L. Qi, S. C. Zhang, Q.-K. Xue, and X. C. Ma, Appl. Phys. Lett. **97**, 143118 (2010).
[22] F. Reif, *Fundamentals of Statistical and Thermal Physics* (McGraw-Hill, New York, 1965).
[23] P. Mårtensson, G. Meyer, N. M. Am, E. Kaxiras, and K. C. Pandey, Phys. Rev. B **42**, 7230 (1990).
[24] Y. F. Zhang, J. F. Jia, Z. Tang, T. Z. Han, X. C. Ma, and Q. K. Xue, Surf. Sci. **596**, L331 (2005).
[25] P. Lošťák, Č. Drašar, H. Süssmann, P. Reinshaus, R. Novotný, and L. Beneš, J. Cryst. Growth **179**, 144 (1997).
[26] S. Karamazov, J. Horák, J. Navrátil, and P. Lošťák, Cryst. Res. Technol. **32**, 249 (1997).
[27] H. Ibach and H. Lüth, *Solid-State Physics* (Springer, Berlin, 1995).
[28] T. Plecháček, J. Navrátil, and J. Horák, J. Solid State Chem. **165**, 35 (2002).

Downloaded 30 Dec 2010 to 166.111.26.101. Redistribution subject to AIP license or copyright; see http://apl.aip.org/about/rights_and_permissions